Turbo Trellis-Coded Hierarchical Modulation Assisted Decode-and-Forward Cooperation

Hua Sun, Soon Xin Ng, *Senior Member, IEEE,* and Lajos Hanzo *Fellow, IEEE*

***Abstract*—Hierarchical modulation, which is also known as layered modulation, has been widely adopted across the telecommunication industry. Its strict backward compatibility with single-layer modems and its low complexity facilitate the seamless upgrading of wireless communication services. The potential employment of hierarchical modulation in cooperative communications has the promise of increasing the achievable throughput at a low power consumption. In this paper, we propose a single-relay aided hierarchical modulation based cooperative communication system. The source employs a pair of Turbo Trellis-Coded Modulation schemes relying on specially designed hierarchical modulation, while the relay invokes the Decode-and-Forward protocol. We have analysed the system's achievable rate as well as its bit error ratio using Monte-Carlo simulations. The results demonstrate that the power consumption of the entire system is reduced to 3.62 dB per time slot by our scheme.**

***Index Terms*—Hierarchical Modulation, Turbo Trellis-Coded Modulation, Cooperative Communication, Soft Decoding, Channel Capacity and Power Efficiency.**

I. Introduction

As an integral part of the DVB-T/-H standard [1], Hierarchical Modulation (HM) is widely employed in the telecommunication industry. The HM scheme was originally developed for upgrading diverse telecommunication services, where the new services may be mapped to new layers, while maintaining a strict backward compatibility [2], [3]. Hence, compared to a system using conventional modulation, HM has a higher flexibility, where both the original and the upgraded new services are combined by the HM scheme and broadcast to the upgraded receivers without requiring any additional bandwidth. Moreover, the original legacy devices are still supported by the upgraded broadcast system, but they are unable to receive the upgraded new services without software or hardware upgrade [4].

The attainable Bit Error Ratio (BER) performance and the achievable throughput of the HM scheme have been investigated in [5], [6], while the performance of the HM scheme in cooperative communications had been discussed in [7], [8]. The authors of [9]–[12] had pointed out that the layered structure of the HM scheme may be used for providing Unequal Error Protection (UEP), which ensures that at least the most important information can be received in the presence of a low receive Signal-to-Noise Ratio (SNR). More specifically, the authors of [1], [13], [14] invoke a HM scheme for providing UEP for image encoding, where the information bits are mapped to specific protection layers according to their error-sensitivity based priority. Moreover, the HM scheme has also been combined with sophisticated channel coding schemes in [13]–[15] for the sake of protecting the most important information. The simulation results of HM in [13], [14] have shown that receiving the information having the highest priority requires a lower received SNR (SNR_r) compared to conventional modulation schemes at a given target BER performance. However, the SNR required for receiving the lower protection layer becomes much higher than that of the identical-throughput conventional modulation. Nonetheless, when considering the performance of the HM scheme in cooperative communications, the majority of research contributions documented the performance of HM schemes based on conventional constellations and the relay was assumed to be at a fixed position (often located in the middle of the source-to-destination link), which reduces the power-efficiency and flexibility of the system.

In [16], we have proposed a cooperative communication system assisted by a hierarchical Turbo Trellis-Coded Modulation (TTCM) scheme. The idea is to use the HM scheme to reduce the transmit SNR[1] (SNR_t) of the Source Node (SN) in cooperative communications. However, we observe that the system in [16] has three drawbacks. Firstly, the 'time-efficiency' of the system is relatively low, because the Destination Node (DN) may only be able to decode the information it received from the SN and Relay Node (RN), when all the nodes in the cooperative network have completed their transmission. Secondly, the power-efficiency of the system may be further improved, because in [16] we assume that the SNR_t of the RN (SNR_t^{RN}) is identical to the SNR_t of the SN (SNR_t^{SN}). The reduced path-loss introduced by the RN was not taken into consideration in the simulations, where the RN was located right in the middle of the SN to DN link. Thirdly, we distorted the HM constellation for the sake of improving the BER performance of its high-priority layers at the detriment of its low-priority layers, which degrades its average BER compared to that of conventional modulation schemes.

The authors are with the School of Electronics and Computer Science, University of Southampton, Southampton, SO17 1BJ, U.K. (e-mail: {hs4g09,sxn,lh}@ecs.soton.ac.uk).

The financial support of the European Union's Seventh Framework Programme (FP7/2007-2013) under the auspices of the CONCERTO project (grant agreement no 288502) as well as of the RC-UK under the India-UK Advanced technology Centre and of the European Research Council Advanced Fellow Grant and of the Royal Society's Wolfson Research Merit Award is gratefully acknowledged.

[1]The definition of transmit SNR was proposed in [17], which is convenient for simplifying the discussions, although this is not a physically measurable quantity, because it relates the power at the transmitter to the noise at the receivers

Given all this background, we proposed a new cooperative communication system in this paper, where the RN position is no longer a fixed position. Instead, similar to the user-cooperation philosophy of [18], we will find the optimum RN position. The design goal of the system in this paper is to combine the TTCM channel coding scheme and HM scheme in the context of cooperative communications for the sake of increasing its time-efficiency and for reducing the total power dissipation of the entire system, while maintaining a low complexity and guaranteeing reliable transmission in each link of the cooperative network. The HM constellations and the position of the RN are also taken into consideration, when optimizing the system. To be more specific, the SN will employ two independent rate-1/2 TTCM encoders and HM is used for combining the two independent codewords into HM symbols. According to the symbol-to-bit demapping of the HM scheme, the SNR_r required for decoding the information contained in the higher protection layers is lower than that of the information in the lower protection layers. Therefore, by employing the HM scheme, the SNR_t^{SN} may be reduced to the minimum required value that can 'just' guarantee the successful detection of the base layer (highest priority) of the entire HM based symbol stream at the DN. By contrast, the information in the lower priority layer may be received and retransmitted by the Decode-and-Forward (DAF) based RN. Hence, the entire system requires two Time Slots (TS) for conveying the information from the SN to the DN. Note that each transmission between the SN (or RN) and the DN only deals with a single layer of the twin-layer HM-16QAM signals. In this way, not only the SNR_t^{SN} and SNR_t^{RN} may be reduced, but also the processing complexity of the system may be mitigated.

The TTCM scheme of [19], is a joint coding and modulation arrangement scheme employing a similar structure to that of turbo codes, but employs Trellis-Coded-Modulation (TCM) [20] as its components. Specifically, TTCM is invoked as the coding and modulation scheme in our communication system, because it has a better performance when communicating over Rayleigh fading channels than that of other joint coding and modulation schemes, such as TCM and Bit-Interleaved Coded Modulation (BICM), as well as iteratively detected BICM (BICM-ID) [19]. An excellent performance is achieved without expanding the bandwidth for the sake of accommodating channel coding. Furthermore, our rate-1/2 TTCM is compatible with HM, since for each HM layer we have two bits, and similarly, the output codeword of the rate-1/2 TTCM encoder also contains two bits. Hence, if we want to reserve one bit of a HM layer for the redundancy bit to protect the original information bits, the TTCM encoder directly satisfies this requirement.

The main contributions of this paper are as follows:

- A new HM scheme is designed for DAF based cooperative communications, which is intrinsically amalgamated with TTCM and we refer to it as Turbo Trellis-Coded Hierarchical Modulation (TTCHM);
- The capacity lower bound of our DAF cooperative system is derived based on the Discrete-input Continuous-output Memoryless Channel (DCMC) capacity analysis, as well as on the DCMC capacity of each individual layer of the twin-layer HM-16QAM symbol sequence;
- Based on the DCMC capacity analysis and on our Monte-Carlo simulations, a power allocation plan is provided and it is demonstrated that the power dissipation of the entire system may be readily optimized by relying on just two variables, namely the HM ratio R and the DAF RN's position.

The rest of the paper is organized as follows: Section II introduces both our system model and our cooperative communication strategy. Section III illustrates the HM scheme proposed for cooperative communications, and details the symbol-to-bit demapper of the HM symbols. The DCMC capacity analysis and our optimization procedure are described in Sections IV. In Sections V, the proposed TTCHM aided cooperative system is investigated and our power-allocation plan is characterized. Our conclusions and future research are discussed in Section VI.

II. System Model

The general model of our TTCHM aided DAF RN based cooperative communication system is depicted in Fig. 1. During the first transmission TS, a sequence of TTCHM symbols $\{x_s\}$ is broadcast by the SN to both the RN and the DN. The SNR_t^{SN} is set to the minimal value for enabling the DN to decode only the information contained in the first layer L_1 (base layer) of the TTCHM signals $\{x_s\}$. Then in the following TS, another signal frame, namely $\{x_r\}$ is forwarded to the DN by the RN. The DN would then be capable of recovering the second layer L_2 of the signal frame $\{x_s\}$ based on the signal sequence received from the RN. In order to simplify the system, we consider that the position of the RN is located between the direct SN-DN path.

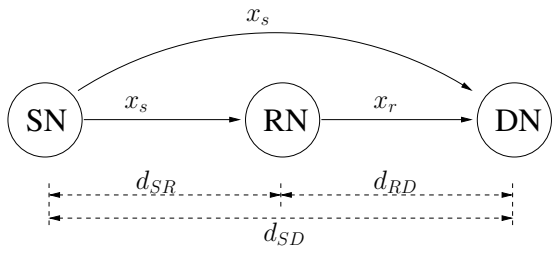

Fig. 1. The model of a single-relay cooperative system.

We considered an uncorrelated Rayleigh flat-fading channel, where the receivers were assumed to acquire perfect Channel State Information (CSI). After the first TS, each symbol received by the DN may be expressed as:

$$y_{SD} = \sqrt{G_{SD}} h_{SD} x_s + n_{SD} \ , \tag{1}$$

while each of the symbols received by the RN is:

$$y_{SR} = \sqrt{G_{SR}} h_{SR} x_s + n_{SR} \ , \tag{2}$$

where the subscript SD denotes the SN-DN link and the subscript SR represents the SN-RN link. By contrast, each of

the symbols received at the DN during the second TS, which are sent by the RN, may be expressed as:

$$y_{RD} = \sqrt{G_{RD}} h_{RD} x_r + n_{RD} \ , \tag{3}$$

where the subscript RD represents the RN-DN link. Additionally, the notations h_{SD}, h_{SR} and h_{RD} denote the complex-valued coefficients of the uncorrelated Rayleigh fading for the different links, while n_{SD}, n_{SR} and n_{RD} denote the Additive White Gaussian Noise (AWGN) having a variance of $N_0/2$ per dimension. Moreover, the variables G_{SD}, G_{SR} and G_{RD} represent the Reduced-Distance-Related-Pathloss-Reduction (RDRPLR) for each link, which we also refer to as the path-gain. We consider an inverse-second-power law based free-space path-loss model [17], [21] and naturally, the path-gain G_{SD} of the SD link is assumed to be unity. Therefore the path-gain of the SR link is [22]:

$$G_{SR} = \left(\frac{d_{SD}}{d_{SR}} \right)^2 \ , \tag{4}$$

and similarly, the path-gain of the RD link is:

$$G_{RD} = \left(\frac{d_{SD}}{d_{RD}} \right)^2 \ , \tag{5}$$

while, we also have:

$$d_{SD} = d_{SR} + d_{RD} \ . \tag{6}$$

In a realistic situation, there is always a path-loss between the SN and DN, but in order to simplify the system model, in our simulations, we normalized this path-loss to 0 dB. Hence the transmit power at the SN (which is also referred to as the signal power) would be identical to the power received at the DN. If the transmissions between the SN and DN are on a frame-by-frame basis over the uncorrelated Rayleigh fading channel, the average received SNR$_r$ ($\overline{SNR_r^{DN}}$) at the DN would be given by:

$$\overline{SNR_r^{DN}} = E(|h|^2 \, SNR_t) = E(|h|^2) SNR_t^{SN} \ , \tag{7}$$

where SNR$_t^{SN}$ is the transmit SNR defined as the ratio of the transmit power at the SN to the noise power at the DN:

$$SNR_t^{SN} = \frac{E(|x|^2)}{N_0} = \frac{1}{N_0} \ , \tag{8}$$

with $E(|x|^2) = 1$. Furthermore, the uncorrelated Rayleigh fading coefficient h is generated by the complex-valued Gaussian distribution having a zero mean and a variance of one. When the number of uncorrelated Rayleigh fading coefficients we generated is large, we have [23]:

$$E(|h|^2) = \frac{1}{N} \sum_{k=1}^{N} |h_k|^2 \approx 1 \ . \tag{9}$$

Hence, for a large frame size of N symbols, we may assume that the SNR$_r$ (SNR$_r^{DN}$) at the DN is equal to SNR$_t^{SN}$, or equivalently $\overline{SNR_r^{DN}} = SNR_t^{SN}$.

To be more specific, the block diagram of the entire system is shown in Fig. 2. If the SNR$_r$ at DN (SNR$_r^{DN}$) is not high enough, the DN may opt for decoding the information only from Encoder 1 during the first TS. During the second TS, the RN is expected to send the information from Encoder 2 to the DN. Additionally, the RN here would demodulate all bits of the HM-16QAM symbols, but it only has to decode the information received from Encoder 2, regardless of the information gleaned from Encoder 1 and encapsulated in the HM-16QAM symbol. The RN would hence re-encode the information corresponding to Encoder 2, and then the encoded signal would be mapped onto a conventional square 4QAM symbol for transmission to the DN.

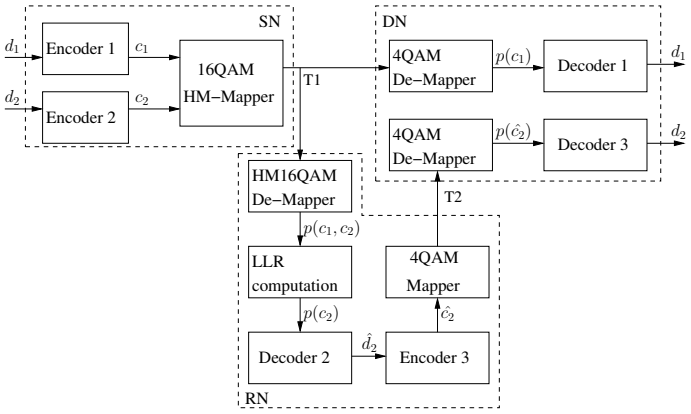

Fig. 2. The system diagram of a single-relay aided cooperative system.

III. Twin Layer HM Modulation

Our twin-layer model of the HM-16QAM constellation seen in Fig. 3 was originally introduced in [16]. Since TTCM is employed, where the symbol-based decoder's performance is determined by the Symbol Error Ratio (SER) [19], set-partition based bit-to-symbol mapping is invoked by the HM constellation instead of Gray mapping.

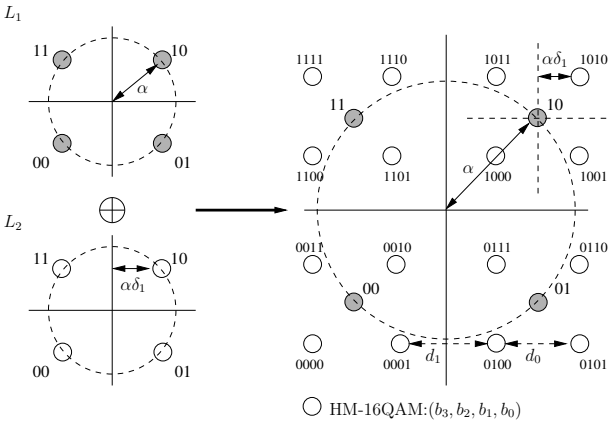

Fig. 3. The constellation map of the HM scheme, where $R = d_1/d_0$.

We define the four bits in a HM-16QAM symbol as $(b_3 b_2 b_1 b_0)$, where L_1 is occupied by $(b_3 b_2)$, while $(b_1 b_0)$ are contained in L_2. The generation rule of the twin-layer HM-16QAM symbols may be expressed as:

$$S_{HM-16QAM} = \alpha \left[S_{4QAM} \pm \sqrt{2} \delta_1 e^{\pm \frac{\pi}{4} j} \right] \ , \tag{10}$$

where S_{4QAM} denotes the conventional square 4QAM constellations, while the parameter α is used for normalizing

the average symbol energy to unity. Furthermore, the ratio $R = d_1/d_0$ is defined for controlling the shape of the HM-16QAM constellations, as shown in Fig. 3, where both the parameters α and δ_1 are directly controlled by the HM ratio R and their relationship may be expressed as follows:

$$\delta_1 = \frac{1}{\sqrt{2}\,(1+R)} \ . \tag{11}$$

$$\alpha = \frac{1}{\sqrt{1+2\delta_1^2}} = \frac{1+R}{\sqrt{1+(1+R)^2}} \ . \tag{12}$$

Finally, another constraint is imposed on the HM ratio R in the simulations, namely that $R > 0$, as detailed in [16]. The entire HM-16QAM constellation point arrangement is directly controlled by the HM ratio R. Upon increasing the value of R, the four constellation points in each quadrant would move closer to each other. Hence it is necessary to have a higher SNR_r at the RN (SNR_r^{RN}) in order to adequately detect the information contained in L_2. However, we only need a lower SNR_r^{DN} for a reliable[2] detection of the two bits in L_1 at DN. Again, in this paper, our objective is to find the optimum HM ratio and the related RN position.

A. L_1 Detection at DN

When SNR_t^{SN} is relatively low, DN is only capable of receiving the information contained in L_1 of the signal sequence it received from the SN. Hence, DN may demap the HM-16QAM signal frames as 4QAM symbols for detecting L_1. The input to the TTCM decoder is an $(N \times M)$-element probability matrix, where N is the number of received symbols, which equals to the block size η of the encoder and M is the number of modulation levels. The element in the matrix is the probability of $\Pr\left(x_n^{(i)} \middle| y\right)$, where y is the received signal, while $x_n^{(i)}$ is the hypothetically transmitted M-ray symbol for $i \in \{0, 1, \cdots, M-1\}$ and n is the time index, which denotes the order of the current received symbol in the signal frame received. In order to decode L_1 at the DN, the demapper should produce an $(N \times 4)$-element Probability Density Function (PDF) matrix of $p(y|x_n^{(i)})$. According to (10), the elements of the PDF matrix may be expressed as:

$$p\left(y_{SD}|x_{q,n}^{(i)}\right) = \frac{1}{\pi N_0} \exp\left(-\frac{|y_{SD} - \sqrt{G_{SD}} h x_{q,n}^{(i)}|^2}{N_0}\right)$$
$$x_{q,n}^{(i)} \in \{\alpha e^{j-3\pi/4}, \alpha e^{j-\pi/4}, \alpha e^{j\pi/4}, \alpha e^{j3\pi/4}\}. \tag{13}$$

This $(N \times 4)$-element PDF matrix is used for computing the input of Decoder 1 as: [19]

$$\Pr\left(L_{1,n}^i|y_{SD}\right) = p\left(y_{SD}|x_{q,n}^{(i)}\right) \Pr\left(x_{q,n}^{(i)}\right) \ , \tag{14}$$

where $i \in \{0, 1, 2, 3\}$ and $n \in \{0, 1, \cdots, \eta - 1\}$, while $\Pr\left(x_{q,n}^{(i)}\right) = 1/4$, which represents equi-probable symbols because we do not consider iterative detection exchanging extrinsic information with the demapper in our symbol-based scheme. When demapping the HM-16QAM signal to 4QAM symbols for calculating the conditional PDF of receiving L_1, we will assume the signal sequence that DN received during the first TS to be 4QAM symbols. Let L_1^0 represent the pair of bits (00) in L_1, L_1^1 for (01), L_1^2 for (10) and L_1^3 for (11), while the positions of the constellation points of x_q here are the four center points in each quadrant, which are shown in Fig. 3.

[2]We define a 'reliable detection' as a detection that gives BER lower than 10^{-6}.

B. L_2 Detection at RN

As shown in Fig. 2, RN receives and retransmits the information in L_2, where SNR_r^{DN} has to be sufficiently high to guarantee that the RN is capable of receiving the entire HM-16QAM signal sequence from the SN. During the first TS, the RN will firstly demap the HM-16QAM signal received from SN to produce an $(N \times 16)$-element PDF matrix, where according to the HM-16QAM generation rule, the elements in the $(N \times 16)$ PDF matrix may be expressed as:

$$p\left(y_{SR}|\, x_{s,n}^{(i)}\right) = \frac{1}{\pi N_0} \exp\left(-\frac{|y_{SR} - \sqrt{G_{SR}} h x_{s,n}^{(i)}|^2}{N_0}\right)$$
$$x_{s,n}^{(i)} \in \{\alpha \left[S_{4QAM} \pm \sqrt{2}\delta_1 e^{\pm\frac{\pi}{4}j}\right]\} \ . \tag{15}$$

Then, the $(N \times 16)$-element probability matrix of $\Pr(x_{s,n}^{(i)}|y_{SR})$ may be derived by:

$$\Pr\left(x_{s,n}^{(i)}\middle|\, y_{SR}\right) = p\left(y_{SR}|\, x_{s,n}^{(i)}\right) \Pr\left(x_{s,n}^{(i)}\right) \ , \tag{16}$$

where $i \in \{0, 1, 2, \cdots, 15\}$, $n \in \{0, 1, \cdots, \eta - 1\}$, while $\Pr\left(x_{s,n}^{(i)}\right) = 1/16$, which represents equi-probable symbols. The Log Likelihood Ratio (LLR) computation block (as shown in Fig. 2) will generate the probability matrix of the information in L_2 gleaned from the HM-16QAM symbol it received. The resultant generation rule is given by:

$$\begin{aligned}\Pr\left(L_{2,n}^l\middle|\, y_{SR}\right) = &\Pr\left(x_{s,n}^{(l)}\middle|\, y_{SR}\right) + \Pr\left(x_{s,n}^{(l+4)}\middle|\, y_{SR}\right) + \\ &\Pr\left(x_{s,n}^{(l+8)}\middle|\, y_{SR}\right) + \Pr\left(x_{s,n}^{(l+12)}\middle|\, y_{SR}\right) \\ &l \in \{0, 1, 2, 3\}, \quad n \in \{0, 1, \cdots, \eta - 1\} \ ,\end{aligned} \tag{17}$$

where, we have $\{x_s^{(0)} = (0000), x_s^{(1)} = (0001), \cdots, x_s^{(15)} = (1111)\}$ and $\Pr\left(L_{2,n}^l\middle|\, y_{SR}\right)$ denotes the elements in the $(N \times 4)$-element probability matrix, which is the input of Decoder 2, generating L_2. After decoding the information in L_2, the RN will then re-encode the information and retransmit them to DN in the following TS using the rate-1/2 TTCM 4QAM scheme.

C. Approximate-Log-MAP Algorithm

The soft information will be used by the Maximum A Posteriori (MAP) algorithm [19] based TTCM decoder. In order to reduce the complexity of the MAP algorithm in the iterative decoding, we employ the Approximate-Log-MAP scheme in our simulations, which was developed from the Max-Log-MAP scheme. The Max-Log-MAP scheme simplifies the MAP algorithm by converting its operation to the logarithmic domain and by using the approximation [19]:

$$\ln\left(\sum_n e^{s_n}\right) \approx \max_n\left(s_n\right) \ , \tag{18}$$

where $\max_n(s_n)$ denotes the maximum value of $\{s_n\}$ for all n. By contrast, the approximate-Log-MAP algorithm exploits that:

$$\begin{aligned}\ln\left(e^{s_1}+e^{s_2}\right) &= \max(s_1,s_2)+\ln\left(1+e^{-|s_1-s_2|}\right)\\ &= \max(s_1,s_2)+f_c\left(|s_1-s_2|\right)\\ &= g(s_1,s_2)\ ,\end{aligned} \tag{19}$$

where the values of the function f_c may be found in a look-up table introduced in [24]. Hence (18) may be converted to:

$$\ln\left(\sum_n e^{s_n}\right) = g\left\{s_n, g\left(s_{n-1},\cdots g\left[s_3, g\left(s_1,s_2\right)\right]\cdots\right)\right\}\ . \tag{20}$$

By applying a look-up table, the approximate-Log-MAP algorithm's complexity is reduced. Hence, it is only slightly more complex than the Max-Log-MAP, but has a similar performance to that of the MAP algorithm.

IV. DCMC BASED SYSTEM ANALYSIS

The achievable DCMC capacity will be used for calculating both the bound of our cooperative communication system, as well as the achievable rate of receiving L_1 and L_2 from the twin-layer HM-16QAM symbols. When considering the DCMC capacity with input $X=\{x^{(0)},x^{(1)},\ldots,x^{(M-1)}\}$ (M is constellation size) and output $Y=\mathbb{C}$, the PDF of receiving y given that $x^{(k)}$ is transmitted may be expressed as [25]:

$$p(y|x^{(k)}) = \frac{1}{\pi N_0}\exp\left(\frac{-||y-hx^{(k)}||^2}{N_0}\right)\ , \tag{21}$$

where we have:

$$p(y) = \sum_{k=0}^{M-1} p(y|x^{(k)})\Pr(x^{(k)})\ , \tag{22}$$

here Pr is for probability. To elaborate further, the mutual information of receiving y when $x^{(k)}$ is transmitted is given by $\log_2[p(y\mid x^{(k)})/p(y)]$, hence the average mutual information of receiving the output Y due to the input X may be derived as [25], [26]:

$$I(X;Y) = \sum_{i=0}^{M-1}\int_{-\infty}^{+\infty} p(y|x^{(i)})\Pr(x^{(i)})\log_2\left(\frac{p(y|x^{(i)})}{\sum_{k=0}^{M-1}p(y|x^{(k)})\Pr(x^{(k)})}\right)\mathrm{d}y\ . \tag{23}$$

So the DCMC capacity can be formulated as:

$$C_{DCMC}^{ML} = \max_{\Pr(x^{(i)})} I(X;Y)\ , \tag{24}$$

where ML is short for maximum likelihood, $I(X;Y)$ is maximized when we have $\Pr(x^{(i)})=1/M$ $(i\in\{0\sim M-1\})$ and (24) may be simplified as [25]:

$$C_{DCMC}^{ML} = \log_2(M) - \frac{1}{M}\sum_{i=0}^{M-1} E\left[\log_2\sum_{k=0}^{M-1}\exp(\Phi_{i,k})\mid x^{(i)}\right]\ , \tag{25}$$

where the unit of C is bits per symbol (bps). Furthermore, $E[A\mid x^{(i)}]$ is the expectation of A conditioned on $x^{(i)}$, whereas the term $\Phi_{i,k}$ may be expressed similarly to that in [25]:

$$\Phi_{i,k} = \frac{-\left\|\sqrt{G}h(x^{(i)}-x^{(k)})+n\right\|^2+\|n\|^2}{N_0}\ , \tag{26}$$

where h is the fading coefficient, G is the path-gain and n is the AWGN at the receiver. In this paper, the DCMC capacity will be used for deriving the lower bound of the entire cooperative communication system, as well as the achievable performance of receiving each layer of the HM signals. The E_s/N_0 difference between the simulation results and the DCMC capacity is our key performance metric, because it explicitly characterizes the ability of our TTCHM scheme to approach the idealized DCMC capacity.

A. Channel Capacity of the SN-DN Link

In our communication protocol, the DN demaps the HM-16QAM symbols received from the SN during the first TS as 4QAM symbols for decoding the information contained in L_1 of the HM signals. Therefore, when calculating the DCMC capacity of the SN-DN link, the constellation size here would be set to $M=4$, rather than to $M=16$. By contrast, the signal received over the SN-DN link is the HM-16QAM symbol stream. Therefore we have to evaluate the DCMC capacity of the 4QAM partition of our HM-16QAM constellation. We choose those four center points (αS_{4QAM}), as shown in Fig. 3, in each quadrant to calculate the DCMC capacity lower bound of receiving L_1 from the HM-16QAM symbols, which hence will be referred to as the capacity of L_1:

$$C_{HM-16QAM}^{L_1} = 2-\frac{1}{4}\sum_{i=0}^{3} E\left[\log_2\sum_{k=0}^{3}\exp(\Phi_{i,k})\mid x_q^{(i)}\right]\ , \tag{27}$$

where we have $x_q^{(i)}\in\{\alpha e^{j\pi/4},\alpha e^{j3\pi/4},\alpha e^{j-3\pi/4},\alpha e^{j-\pi/4}\}$, $i\in\{0,1,2,3\}$ and α is the normalized polynomial of the HM-16QAM symbols based on the current HM ratio.

B. Channel Capacity of the SN-RN Link

The RN would demap the signal received from the SN by the HM-16QAM demapper of Fig. 2 and calculates a $(N\times 16)$-element symbol probability matrix, if the RN is used for receiving both of the two layers' information in the HM symbol, the channel capacity may be expressed as:

$$C_{HM-16QAM} = 4-\frac{1}{16}\sum_{i=0}^{15} E\left[\log_2\sum_{k=0}^{15}\exp(\Phi_{i,k})\mid x_s^{(i)}\right]\ , \tag{28}$$

where we have $x_s^{(i)}\in\{\alpha\left[S_{4QAM}\pm\sqrt{2}\delta_1 e^{\pm\frac{\pi}{4}j}\right]\}$ and $i\in\{0,1,2,\cdots,15\}$. However, the RN will only deal with the information in L_2, while the $(N\times 16)$-element probability matrix will be converted into a $(N\times 4)$-element matrix for decoding the information in L_2 of the HM symbols. When considering the DCMC capacity of receiving L_2 of the HM signal, we also have to subtract two bits from the DCMC capacity of the HM-16QAM constellation. Hence, based on

the chain-rule of mutual information [19], [26], we have:

$$\begin{aligned}
&I(b_3, b_2, b_1, b_0; y) \\
&= I(b_3; y) + I(b_2; y \mid b_3) + I(b_1; y \mid b_3, b_2) + I(b_0; y \mid b_3, b_2, b_1) \\
&= [H(b_3) + H(b_2 \mid b_3)] - [H(b_3 \mid y) + H(b_2 \mid b_3, y)] + \\
&\quad [H(b_1 \mid b_3, b_2) + H(b_0 \mid b_3, b_2, b_1)] - \\
&\quad [H(b_1 \mid b_3, b_2, y) + H(b_0 \mid b_3, b_2, b_1, y)] \\
&= H(b_3, b_2) - H(b_3, b_2 \mid y) + H(b_1, b_0 \mid b_3, b_2) - \\
&\quad H(b_1, b_0 \mid b_3, b_2, y) \\
&= I(b_3, b_2; y) + I(b_1, b_0; y \mid b_3, b_2) \ , \qquad (29)
\end{aligned}$$

while $H(X, Y)$ is the joint entropy given by

$$H(X, Y) = -\sum_{x \in X} \sum_{y \in Y} p(x, y) \log_2 p(x, y). \qquad (30)$$

It can be stated that:

$$I(b_1, b_0; y \mid b_3, b_2) = I(b_3, b_2, b_1, b_0; y) - I(b_3, b_2; y) \ , \quad (31)$$

where we have $C_{HM-16QAM} = \max_{\Pr(x_s)} \{I(b_3, b_2, b_1, b_0; y)\}$, which is the DCMC capacity of receiving HM-16QAM signals, while $C^{L_1}_{HM-16QAM} = \max_{\Pr(x_q)} \{I(b_3, b_2; y)\}$, which is the DCMC capacity of receiving L_1 from the twin-layer HM-16QAM signal. When considering $I(b_1, b_0; y \mid b_3, b_2)$, we found that the detection of L_2 is not entirely independent from the information contained in L_1. However, the achievable DCMC capacity of receiving L_2 will only be approached, when L_1 is perfectly received. Hence, we may define the DCMC capacity of receiving L_2 to be $C^{L_2}_{HM-16QAM} = \max_{\Pr(x_s)} \{I(b_1, b_0; y \mid b_3, b_2)\}$, which may be expressed as:

$$C^{L_2}_{HM-16QAM} = C_{HM-16QAM} - C^{L_1}_{HM-16QAM} \ . \qquad (32)$$

Note that the average symbol power is normalized to unity, and the HM-16QAM symbols are equi-probable, hence $\Pr(x_q) = 1/4$ and $\Pr(x_s) = 1/16$.

C. Overall system optimization based on DCMC capacity

In our simulations, the coding rate of the two encoders employed by the SN is 1/2, hence we only focus our attention on the specific SNR values, where the DCMC capacity reaches 1 bps. Multiple values of the HM ratio had been tested. At a given HM ratio, both the minimum $SNR^{L_1}_r$ required for decoding L_1 at the DN and $SNR^{L_2}_r$ of decoding L_2 at the RN may be found. The SNR difference between the two layers is:

$$\mathcal{G}_{SNR} = SNR^{L_2}_r - SNR^{L_1}_r \ [\text{dB}] \ . \qquad (33)$$

If we set SNR^{SN}_t to be identical to the specific SNR_r value, which is required for the reliable detection of L_1 in the HM-16QAM symbol, we may have $SNR^{SN}_t = SNR^{L_1}_r$. This would guarantee that the BER of decoding L_1 would reach an arbitrarily low value. In this situation, if we want the BER performance of receiving L_2 to become sufficiently low, the channel gain G_{SR} of the SN-RN link should satisfy:

$$10 \log_{10} G_{SR} + SNR^{L_1}_r = SNR^{L_2}_r \ . \qquad (34)$$

If we use the ratio d_{SR}/d_{SD} for representing the position of the RN, we arrive at:

$$\mathcal{G}_{SNR} = 10 \log_{10} \left(\frac{d_{SD}}{d_{SR}} \right)^2 \ , \qquad (35)$$

where $\mathcal{G}_{SNR}$ is given by (33) and hence we have:

$$\frac{d_{SR}}{d_{SD}} = 10^{-\frac{\mathcal{G}_{SNR}}{20}} \ . \qquad (36)$$

Once the position of the RN becomes known, the path gain between the RN and DN is formulated as:

$$G_{RD} = \left(1 - \frac{d_{SR}}{d_{SD}} \right)^{-2} \ . \qquad (37)$$

In the capacity analysis, we observe that a system employing a rate-1/2 channel coding scheme and 4QAM modulation for communication over uncorrelated Rayleigh fading channels requires $SNR_r = 1.81$ dB to reach a DCMC capacity of 1 bps. Hence the SNR^{RN}_t has to satisfy:

$$SNR^{RN}_t = 1.81 - 10 \log G_{RD} \quad [\text{dB}] \ . \qquad (38)$$

Likewise, the SNR^{SN}_t of the SN should guarantee that:

$$SNR^{SN}_t = SNR^{L_1}_r \ . \qquad (39)$$

Hence, the average SNR_t of the entire system is given by:

$$\overline{SNR_t} = 10 \log_{10} \left(\frac{10^{(SNR^{SN}_t/10)} + 10^{(SNR^{RN}_t/10)}}{2} \right) \quad [\text{dB}] \ . \qquad (40)$$

Let us now consider the DCMC capacity at the HM ratio of $R = 1.5$ for instance. Based on (27) and (32), the DCMC capacity of receiving L_1, L_2 and conventional 4QAM relying on Gray mapping for transmission over uncorrelated Rayleigh fading channels are shown in Fig. 4(a). Observe from Fig. 4(a) that the SNR_r values required for the reliable detection of L_1 and L_2 of our rate-1/2 coded HM-16QAM scheme are 2.46 dB and 11.41 dB, respectively. Hence, SNR^{SN}_t should be set to 2.46 dB and the path-loss reduction of the SN-RN link is $11.41 - 2.46 = 8.95$ dB. Given the path gains G_{SR} and G_{RD}, the DCMC capacity based on the SNR_t of L_1 and L_2 is portrayed in Fig. 4(b). Observe in Fig. 4(b) that there is an intersection between the DCMC capacity curves of L_1 and L_2. This intersection indicates that an arbitrarily low BER can be achieved at the DN (for L_1) and at the RN (for L_2), provided that the SNR^{SN}_t is at least 2.46 dB. Note furthermore that with the benefit of having the above-mentioned path gain of 3.88 dB for the RN-DN link, SNR^{RN}_t should be set to $1.81 - 3.88 = -2.07$ dB, in order to achieve a DCMC capacity of 1 bps at the DN. Hence, in this situation, $\overline{SNR_t}$ of the system would be 0.77 dB according to (40). This $\overline{SNR_t}$ value determines the lower bound of the power consumption for our communication strategy based on the current value of the HM ratio R, provided that a perfect capacity-achieving channel coding scheme is used.

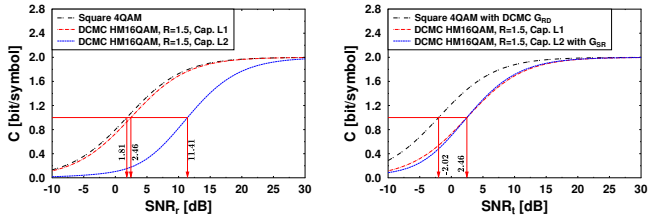

(a) The DCMC capacity versus SNR_r of L_1 and L_2 of our HM-16QAM scheme when the HM ratio R is 1.5, and conventional 4QAM with Gray mapping.

(b) The DCMC capacity versus transmit SNR_t of L_1 and L_2 of our HM-16QAM scheme when the HM ratio R is 1.5, and conventional 4QAM with Gray mapping.

Fig. 4. The figure of DCMC capacity versus SNR. The simulation is based on (22), (27) and (33), and the number of samples when calculating the DCMC capacity is 100k. The channel is uncorrelated Rayleigh fading channel.

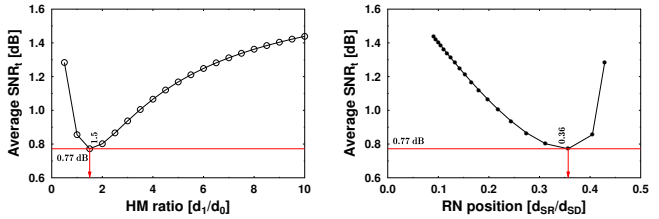

(a) The DCMC based $\overline{SNR_t}$ of the entire system versus HM ratio based on the optimized curve in Fig. 5.

(b) The DCMC based $\overline{SNR_t}$ of the entire system versus RN position based on the optimized curve in Fig. 5.

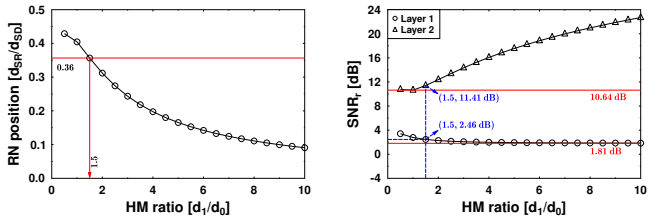

(c) The DCMC based RN position versus HM ratio based on the optimized curve in Fig. 5.

(d) The SNR versus HM ratio figure for decoding L_1 and L_2, the SNR_r here is the value when the DCMC capacity reaches to 1 bps.

Fig. 6. The DCMC capacity analysis based results. The simulation is based on (22), (27) and (35), and the number of samples when calculating the DCMC capacity is 100k. The channel is uncorrelated Rayleigh fading channel.

D. DCMC capacity based results

By calculating the $\overline{SNR_t}$ of multiple HM ratios and on different RN positions, the resultant three-dimensional $\overline{SNR_t}$ versus R and d_{SR}/d_{SD} plot shown in Fig. 5 may be generated. The dashed-line curve seen at the 'valley' in the figure represents the optimized solution based on the current HM ratio R, which is indeed at the lowest point of the power-dissipation surface, confirming that based on a given HM ratio R, our power-allocation regime has found the optimum RN position for ensuring that the power efficiency of the entire system is optimized. Moreover, the value of the HM ratio R will be adjusted according to the current SNR_t^{SN} in order to guarantee the required target BER performance of receiving the information contained in L_1 of the HM-16QAM signal frame. Explicitly, the resultant system is dynamically optimized based on the current SNR_t^{SN}.

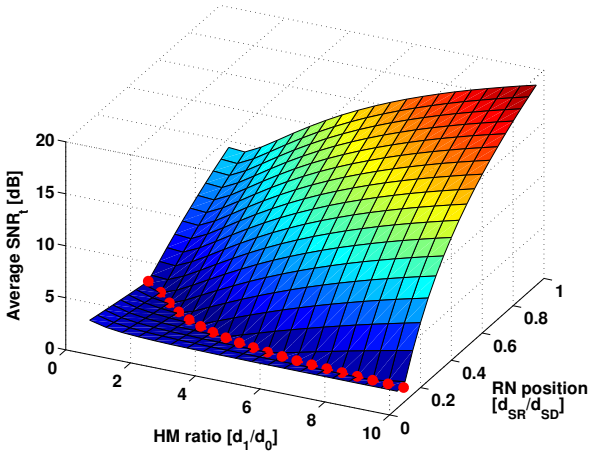

Fig. 5. The 3D plot of the DCMC based power consumption surface of the entire system when using perfect capacity-achieving codes. The simulation is based on (22), (27) and (35), and the number of samples when calculating the DCMC capacity is 100k. The channel is uncorrelated Rayleigh fading channel.

Based on the optimum power consumption curve seen in Fig. 5, we have generated Fig. 6(a) to Fig. 6(c). It can be observed from Fig. 6(a) that when the value of the HM ratio is $R = 1.5$, the $\overline{SNR_t}$ value of the entire system will be 0.77 dB per TS, which is the lowest possible value. This shows that if a perfect capacity-achieving rate-1/2 channel coding scheme is invoked, the optimum power consumption of the entire system will translate into $\overline{SNR_t} = 0.77$ dB per TS, which is considered to be the lower bound of our cooperative communication system. At the same point the optimum position for the RN is at the normalized distance of $d_{SR}/d_{SD} = 0.36$, as also seen in Fig. 6(b). Hence the RDRPLR G_{RD} is 3.88 dB. Furthermore, Fig. 6(c) illustrates that upon increasing the HM ratio R, the optimum position of the RN is moved closer to the SN, which is due to the increase of the SNR_r^{RN} required for adequately receiving L_2, and hence the SNR_t^{RN} required for high-integrity transmissions in the RN-DN link will consequently be increased.

Fig. 6(d) shows the relationship between the required SNR_r and the HM ratios, where we observe that for a reliable detection of the information contained in L_1 of the HM-16QAM scheme, the minimum SNR_r should be higher than 1.81 dB. On the other hand, the lowest SNR_r required for a reliable detection of L_2 is 11.41 dB. Hence, provided that SNR_t^{SN} is higher than 1.81 dB, the system is capable of operating at a vanishingly low BER. Additionally, if SNR_t^{SN} is higher than 11.41 dB, the DN becomes capable of detecting the information received from the SN without the need of employing a RN.

V. TTCHM-16QAM COOPERATIVE SYSTEM DESIGN

In Section IV, we have detailed the DCMC capacity analysis of our cooperative communication strategy and we have found both the minimum power consumption and the optimum RN position. In practice, we do not have any control over the position of mobile relays, but the relay-selection algorithm

would appoint a relay close to the optimum location. In this section, the SN will employ a pair of rate-1/2 TTCM encoders, rather than assuming a perfect capacity-achieving channel code, and we will optimize this practical system.

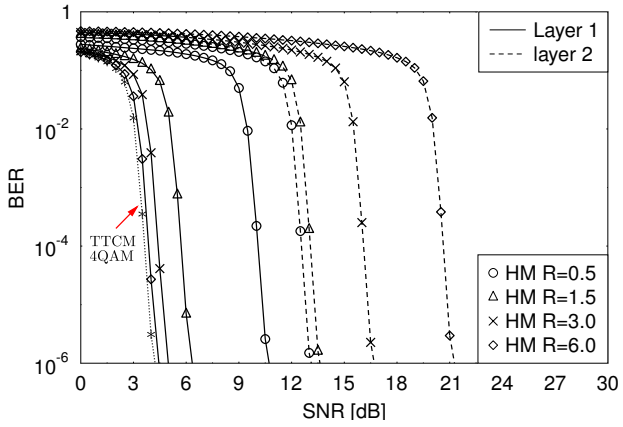

Fig. 7. The BER versus SNR of decoding the information contained in L_1 and L_2 from the HM-16QAM symbols based on different HM ratio R. The SN employs two independent rate-1/2 TTCM encoders with HM-16QAM scheme, while the number of iterations of the decoder is $\zeta = 4$, the block size is $\eta = 12,000$ and the channel is uncorrelated Rayleigh fading channel.

In order to establish a database for the system, we firstly simulated the BER versus SNR performance of both L_1 and L_2 of the HM-16QAM scheme based on different values of the HM ratio R. The results of four typical HM ratio values are shown in Fig. 7. In this investigation, the simulations are carried out in a C++ platform, the number of iterations of our rate-1/2 TTCM decoder is $\zeta = 4$, while the block size is $\eta = 12,000$. Using a large number of iterations allows the TTCM decoder to more closely approach capacity, while a large block length assists in avoiding error propagation, but also imposes an increased complexity. When simulating the BER versus SNR results, we find that no substantial BER performance improvement is achieved for more than four iterations or for block sizes above 12,000 symbols.

The constraint of the system is to guarantee the BER performance of each link should be no higher than 10^{-6}. The TTCHM-16QAM aided cooperative communication system optimized in Section IV is used and our simulation results are discussed in the following section. Note however that since Encoder 2 of Fig. 2 used at the RN is linked with a conventional 4QAM modem with rate-1/2 TTCM channel coding scheme, SNR_t^{RN} is given by:

$$SNR_t^{RN} = 4.23 - 10\log_{10} G_{RD} \quad [\text{dB}] \ , \qquad (41)$$

where a SNR_r of 4.23 dB is required for achieving a BER of 10^{-6} for our TTCM/4QAM single link.

A. Simulation Results

Similar to Fig. 5, the three-dimensional plot of the power consumption surface recorded for our TTCHM aided cooperative communication system is depicted in Fig. 8. The dashed line seen at the valley of the surface represents our optimized TTCHM-16QAM system. Based on the dashed line in Fig. 8, three two-dimensional plots are generated, as seen in Fig. 9(a) to Fig. 9(c). Observe that for achieving BER of 10^{-6}, the TTCHM aided cooperative communication system requires at least $\overline{SNR_t} = 3.62$ dB per TS. The optimum RN position is at $d_{SR} = 0.26 d_{SD}$ and the optimum HM ratio is 3.0, while the throughput of our system is 1 bps . Due to employing a realistic channel coding scheme, our TTCHM system would require a $3.62 - 0.77 = 2.85$ dB higher SNR_t than the idealized system of Section IV, which relied on a perfect capacity-achieving channel code operating exactly at the DCMC capacity of each link.

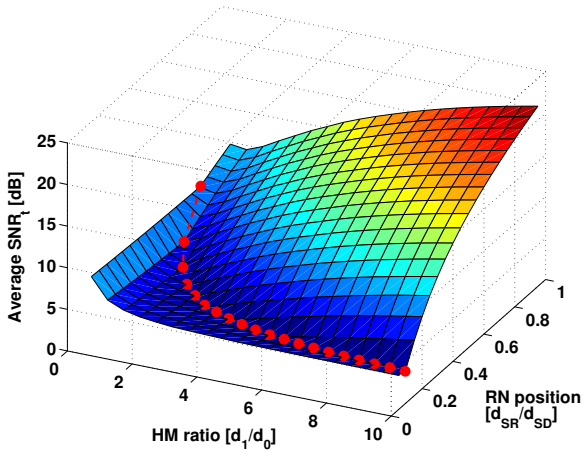

Fig. 8. The 3D plot of the simulation based power consumption surface of the entire system when the SN employs two independent rate-1/2 TTCM encoders with HM-16QAM scheme, while the number of iterations of the decoder is $\zeta = 4$, the block size is $\eta = 12,000$ and the channel is uncorrelated Rayleigh fading channel.

Upon focusing our attention on the BER performance of decoding the information contained in L_1 and L_2 separately, we generated Fig. 9(d). Explicitly, Fig. 9(d) illustrates the relationship between the SNR_r and the related HM ratios required for detecting L_1 and L_2. Based on our optimization regime of Section IV, the discrepancy between the two curves at a given HM ratio may be exploited for deciding upon the required position of the RN. We could also infer two important limits from Fig. 9(d), where the minimum SNR_r required for a reliable detection of the information contained in L_1 is 4.23 dB. This means that based on our communication protocol, it would be impossible for the DN to receive the information of L_1 from the SN at a BER lower than 10^{-6} if SNR_r^{DN} is lower than 4.23 dB. Hence, in this situation the RN would have to be activated to transmit the information of both L_1 and L_2 to the DN. On the other hand, for a reliable detection of L_2, the minimum SNR_r has to be above 12.85 dB, as highlighted in Fig. 9(d). If the SNR_r recorded at the DN is higher than 12.85 dB, the entire system would be turned into a non-cooperative system, because the DN would be capable of decoding the whole HM-16QAM symbol stream at a BER lower than 10^{-6} without invoking a RN.

Note that the throughput of a single link assisted by a rate-1/2 TTCM encoder using 4QAM constellations is also 1 bps, as mentioned at the end of Section V, while the SNR_r required for achieving a BER performance of 10^{-6} by the rate-1/2

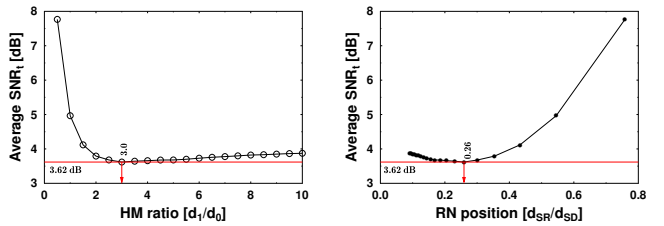

(a) The simulation based average SNR_t of the entire system versus HM ratio based on the optimized curve in Fig. 8.

(b) The simulation based average SNR_t of the entire system versus RN position based on the optimized curve in Fig. 8.

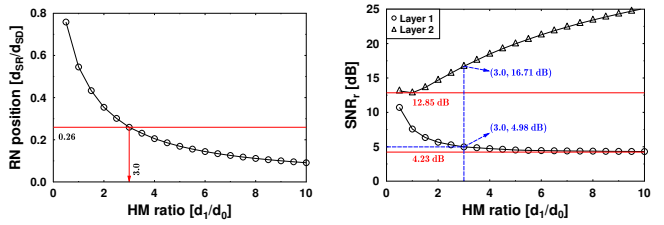

(c) The simulation based RN position versus HM ratio based on the optimized curve in Fig. 8.

(d) The SNR_r versus HM ratio figure for decoding L_1 and L_2, while the value of the SNR_r here is the required SNR_r for each layer to achieve 10^{-6} BER performance.

Fig. 9. The simulation results for our TTCHM-16QAM cooperative communication system, the SN employs two independent rate-1/2 TTCM encoders with HM-16QAM scheme, while the number of iterations of the decoder is $\zeta = 4$, the block size is $\eta = 12,000$ and the channel is uncorrelated Rayleigh fading channel.

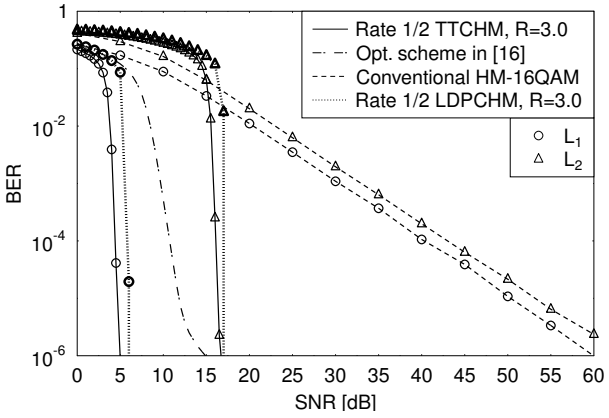

Fig. 10. The BER versus SNR performance of our optimized TTCHM scheme, optimized scheme in [16], the conventional HM scheme and our cooperative system using twin rate-1/2 LDPC encoders. For our optimized TTCHM scheme, the number of iterations of the decoder is $\zeta = 4$, the block size is $\eta = 12,000$ and the HM ratio R is 3.0, and the optimized scheme in [16] employs rate-3/4 TTCM encoder with the same ζ and η. The conventional HM scheme denotes the uncoded HM scheme using conventional 16QAM with Gray mapping. The Rate 1/2 LDPCH denotes the performance of our cooperative system when using twin rate-1/2 LDPC encoders, the block size is $\eta_l = 12,000$ and the max iteration number of the decoder is set to be $\zeta_l = 20$. The channel is uncorrelated Rayleigh fading channel.

TTCM and 4QAM aided scheme is 4.23 dB when communicating over uncorrelated Rayleigh fading channels. Hence, in order to transmit two frames of 4QAM signals, the rate-1/2 TTCM aided single link system will require two TSs, while the $\overline{SNR_t}$ per TS is 4.23 dB, which is 4.23-3.62=0.61 dB higher than that of our TTCHM aided cooperative communication system. Moreover, when the SNR_t^{SN} is higher than 12.85 dB, the throughput of our TTCHM aided cooperative system may be doubled to 2 bps.

The system in [16] has a similar structure to the proposed scheme in this paper and both schemes have to rely on two TSs. However, the scheme in [16] employed a single rate-3/4 TTCM encoder at SN, while at the end of each TS, the DN will only receive two probability matrices. This arrangement does not permit the derivation of the SNR_r required for meeting a specific performance for receiving each of the two layers. Furthermore, the DN in [16] can only start the decoding procedure at the end of the second TS. When comparing the scheme advocated in [16] and the scheme proposed in this paper, it can be observed that even though the throughput of the system in [16] is 1.5 bps, which is higher than the 1 bps throughput of the system in this paper, in this paper we can guarantee that the most important information could be received and decoded immediately after the first TS. Meanwhile, the simulations in [16] were carried out for a fixed RN position (right in the middle of the SN-DN link) and in order to guarantee a BER lower than 10^{-6}, $\overline{SNR_t}$ should be at least 14.89 dB, as shown in Fig. 10. By contrast, the system optimized in this paper requires $\overline{SNR_t} = 3.62$ dB for achieving a BER below 10^{-6}. The optimum RN position is also taken into consideration in the proposed scheme.

When comparing our optimized TTCHM scheme to the conventional HM using uncoded 16QAM relying on Gray mapping, the related simulation results are shown in Fig. 10. It can be observed that for the system using an uncoded HM-16QAM scheme for transmission over the uncorrelated Rayleigh fading channel, the SNR_r^{DN} required for receiving L_1 is above 60 dB, which is approximately 55 dB higher than that of our TTCHM scheme. By contrast, our optimized cooperative TTCHM scheme requires a SNR_t^{SN} of approximately 4.98 dB for achieving a reliable transmission. However, the price we paid for achieving an improved BER performance is the reduction of the system's throughput. When the SNR_t^{SN} is higher than 4.23 dB, but lower than 12.85 dB, the throughput of our cooperative TTCHM system is 1 bps, while if the SNR_t^{SN} is higher than 12.85 dB, the throughput of our cooperative system may reach 2 bps. However, the achievable rate of the conventional HM-16QAM scheme is 4 bps.

Additionally, we have also included the BER versus SNR performance of our cooperative communication system, when using the bit-based rate-1/2 regular LDPC encoder of [27], [28] instead of the symbol-based TTCM scheme. We refer to this LDPC code assisted HM scheme as the LDPCHM arrangement. Here the block size of the rate-1/2 LDPC encoder is the same as that of the TTCM encoder in this paper, while the maximum number of LDPC decoder iterations is set to $\zeta_l = 20$. It can be observed that even though the number of the iterations of the LDPC decoder is significantly higher than that of the TTCM decoder, the BER of L_1 and L_2 of the LDPCHM aided system is still slightly worse than that of the TTCHM scheme. It was also found in [29] that a symbol-based scheme always has a lower convergence threshold than an equivalent bit-based scheme.

VI. Conclusions

In this paper, we have proposed a TTCHM aided cooperative communication system. The system requires 2 TSs for conveying two rate-1/2 TTCM encoded 4QAM signal frames from SN to DN. The optimum $\overline{SNR_t}$ is 3.62 dB per TS, which is within $3.62 - 0.77 = 2.85$ dB of the capacity lower bound. We demonstrated that at a throughput of 1 bps, cooperative communication is capable of providing reliable transmissions, provided that the SNR_t^{SN} is higher than 4.23 dB. By contrast, when SNR_t^{SN} is higher than 12.85 dB, the throughput of the system will be increased to 2 bps, because SNR_t^{SN} becomes high enough for the DN to receive both of L_1 and L_2 from the SN during the first TS. Additionally, invoking more RNs for cooperative communications would allow our system to get closer to the capacity lower bound, but it would inevitably reduce the throughput and increase the system's complexity. As an attractive design alternative, spatial modulation [30] may constitute another technique of approaching the channel capacity, where activating one out of N_t transmit antennas allows us to convey $\log_2 N_t$ extra bits. Hence, for the same throughput, the spatial modulation aided transmitter may employ a lower-order modulation scheme for the activated antenna. This would require a lower SNR_t^{SN} for the classic modulation scheme for achieving the same BER, whilst additionally requiring only a single RF chain. These solutions will be considered in our future investigations.

References

[1] C. Hellge, S. Mirta, T. Schierl, and T. Wiegand, "Mobile TV with SVC and hierarchical modulation for DVB-H broadcast services," *IEEE International Symposium on Broadband Multimedia Systems and Broadcasting, 2009. BMSB '09.*, pp. 1–5, May. 2009.

[2] S. Wang, S. Kwon, and B. K. Yi, "On enhancing hierarchical modulation," *IEEE International Symposium, Broadband Multimedia System and Broadcasting*, pp. 1–6, Jun. 2008.

[3] R. Y. Kim and Y.-Y. Kim, "Symbol-level random network coded cooperation with hierarchical modulation in relay communication," *IEEE Transactions on Consumer Electronics*, vol. 55, pp. 1280–1285, Oct. 2009.

[4] H. Jiang and P. A. Wilford, "A hierarchical modulation for upgrading digital broadcast systems," *IEEE Transactions on Broadcasting*, pp. 223–229, Jun. 2005.

[5] J. Hossain, P. K. Vitthaladevuni, M. S. Alouini, and V. K. Bhargava, "Adaptive hierarchical modulation for simultaneous voice and multiclass data transmission over fading channels," *IEEE Transactions on Vehicular Technology*, vol. 55, pp. 1181–1194, Jul. 2006.

[6] J. Hossain, M. S. Alouini, and V. K. Bhargava, "Rate adaptive hierarchical modulation-assisted two-user opportunistic scheduling," *IEEE Transactions on Wireless Communications*, vol. 6, pp. 2076–2085, Jun. 2007.

[7] M. K. Chang and S. Y. Lee, "Performance analysis of cooperative communication system with hierarchical modulation over Rayleigh fading channel," *IEEE Transactions on Wireless Communications*, vol. 8, pp. 2848 – 2852, Jun. 2009.

[8] S. Y. Lee and K. C. Whang, "A collaborative cooperation scheme using hierarchical modulation," *IEEE 68th Vehicular Technology Conference (VTC)*, pp. 1–5, Sept. 2008.

[9] S. H. Chang, R. Minjoong, P. C. Cosman, and L. B. Mistein, "Optimized unequal error protection using multiplexed hierarchical modulation," *IEEE Transactions on Information Theory*, vol. 58, pp. 5816–5840, Sept. 2012.

[10] Y. J. Noli, H. C. Lee, and L. Y. Lee, "Design of unequal error protection for MIMO-OFDM systems with hierarchical signal constellations," *Journal of Communications and Networks*, vol. 9, pp. 167–176, Jun. 2007.

[11] Y. C. Chang, S. W. Lee, and R. Komiya, "A low complexity hierarchical QAM symbol bits allocation algorithm for unequal error protection of wireless video transmission," *IEEE Transactions on Consumer Electronics*, vol. 55, pp. 1089–1097, Aug. 2009.

[12] K. M. Alajel, W. Xiang, and Y. F. Wang, "Unequal error protection scheme based hierarchical 16-QAM for 3-D video transmission," *IEEE Transactions on Consumer Electronics*, vol. 58, pp. 731–738, Aug. 2012.

[13] S. S. Arslan, P. C. Cosman, and L. B. Milstein, "Coded hierarchical modulation for wireless progressive image transmission," *IEEE Transactions on Vehicular Technology*, pp. 4299 – 4313, Nov. 2011.

[14] S. S. Arslan, P. C. Cosman, and L. B. Milstein, "On hard decision upper bounds for coded m-ary hierarchical modulation," *2011 45th Annual Conference on Information Sciences and Systems (CISS)*, pp. 1–6, Mar. 2011.

[15] C. Hausl and J. Hagenauer, "Relay communication with hierarchical modulation," *IEEE Communications Letters*, vol. 11, pp. 64–66, Jan. 2007.

[16] H. Sun, Y. R. Shen, S. X. Ng, and L. Hanzo, "Turbo trellis coded hierarchical modulation for cooperative communications," *Wireless Communications and Networking Conference (WCNC)*, pp. 2789 – 2794, Apr. 2013.

[17] H. Ochiai, P. Mitran, and V. Tarokh, "Design and analysis of collaborative diversity protocols for wireless sensor networks," *VTC2004-Fall, IEEE 60th Vehicular Technology Coference*, vol. 7, pp. 4645–4649, Sept. 2004.

[18] A. Sendonaris, E. Erkip, and B. Aazhang, "User cooperation diversity Part I and Part II," *IEEE Transactions on Communications*, vol. 51, pp. 1927–1938, Nov. 2003.

[19] L. Hanzo, T. H. Liew, B. L. Yeap, R. Y. S. Tee, and S. X. Ng, *Turbo coding, turbo equalisation and space-time coding : EXIT-chart-aided near-capacity designs for wireless channels*. Wiley-IEEE Press, 2rd ed., 2011.

[20] G. Ungerböck, "Trellis-coded modulation with redundant signal sets. part 1 and 2," *IEEE Communication Magazine*, vol. 25, pp. 5–21, Feb. 1987.

[21] A. Goldsmith, *Wireless Communications*. Cambridge University Press, 1st ed., 2005.

[22] Y. Azar, G. N. Wong, K. wang, and R. Mayzus, "28 GHz propagation measurements for outdoor cellular communications using steerable beam antennas in New York city," *2013 IEEE International Conference on Communications (ICC)*, pp. 5143–5147, Jun. 2013.

[23] S. M. Ross, *Introduction to probability models*. Academic Press., 9th ed., 2007.

[24] P. Robertson, E. Villebrun, and P. Hoeher, "A comparison of optimal and sub-optimal MAP decoding algorithms operating in the log domain," *IEEE International Conference on Communications, 1995. ICC '95 Seattle, 'Gateway to Globalization'*, vol. 2, pp. 1009–1013, Jun. 1995.

[25] S. X. Ng and L. Hanzo, "On the MIMO channel capacity of multidimensional signal sets," *IEEE Transactions on Vehicular Technology*, vol. 55, pp. 528–536, Mar. 2006.

[26] T. M. Cover and J. A. Thomas, *Elements of information theory*. Wiley-Interscience Press, 2rd ed., 2006.

[27] D. J. C. MacKay and R. M. Neal, "Near shannon limit performance of low density parity check codes," *Electronics Letters*, vol. 32, Aug. 1996.

[28] R. G. Gallager, "Low-density parity-check codes," *IRE Transactions on Information Theory*, vol. 8, pp. 21–28, Jan. 1962.

[29] B. Scanavino, G. Montorsi, and S. Benedetto, "Convergence properties of iterative decoders working at bit and symbol level," *IEEE Global Telecommunications Conference, 2001. GLOBECOM'01*, vol. 2, pp. 1037–1041, Nov. 2001.

[30] M. D. Renzo, H. Haas, A. Ghrayeb, S. Sugiura, and L. Hanzo, "Spatial modulation for generalized MIMO: challenges, opportunities, and implementation," *Proceedings of the IEEE*, vol. 102, pp. 56–103, Jan. 2014.

Hua Sun received the B.Eng. degree in electronics and information engineering from the Huazhong University of Science & Technology (HUST), Wuhan, China, in 2009. In 2010, he obtained a MSc degree with distinction in Wireless Communications from the University of Southampton, Southampton, UK. He is currently working towards the PhD degree in the Research Group of Communications, Signal Processing and Control, School of Electronics and Computer Science, University of Southampton, Southampton, UK. His research interests include Superposition Modulation, Hierarchical Modulation, Turbo Trellis-Coded Modulation as well as cooperative communications.

Dr Soon Xin Ng (S'99-M'03-SM'08) received the B.Eng. degree (First class) in electronics engineering and the Ph.D. degree in wireless communications from the University of Southampton, Southampton, U.K., in 1999 and 2002, respectively. From 2003 to 2006, he was a postdoctoral research fellow working on collaborative European research projects known as SCOUT, NEWCOM and PHOENIX. Since August 2006, he has been a member of academic staff in the School of Electronics and Computer Science, University of Southampton. He is involved in the OPTIMIX and CONCERTO European projects as well as the IU-ATC and UC4G projects. He is currently an associate professor in wireless communications at the University of Southampton.

His research interests include adaptive coded modulation, coded modulation, channel coding, space-time coding, joint source and channel coding, iterative detection, OFDM, MIMO, cooperative communications, distributed coding, quantum error correction codes and joint wireless-and-optical-fiber communications. He has published over 180 papers and co-authored two John Wiley/IEEE Press books in this field. He is a Senior Member of the IEEE, a Chartered Engineer and a Fellow of the Higher Education Academy in the UK.

Lajos Hanzo (http://www-mobile.ecs.soton.ac.uk) FREng, FIEEE, FIET, Fellow of EURASIP, DSc received his degree in electronics in 1976 and his doctorate in 1983. In 2009 he was awarded the honorary doctorate "Doctor Honoris Causa" by the Technical University of Budapest. During his 38-year career in telecommunications he has held various research and academic posts in Hungary, Germany and the UK. Since 1986 he has been with the School of Electronics and Computer Science, University of Southampton, UK, where he holds the chair in telecommunications. He has successfully supervised about 100 PhD students, co-authored 20 John Wiley/IEEE Press books on mobile radio communications totalling in excess of 10 000 pages, published 1400+ research entries at IEEE Xplore, acted both as TPC and General Chair of IEEE conferences, presented keynote lectures and has been awarded a number of distinctions. Currently he is directing a 100-strong academic research team, working on a range of research projects in the field of wireless multimedia communications sponsored by industry, the Engineering and Physical Sciences Research Council (EPSRC) UK, the European Research Council's Advanced Fellow Grant and the Royal Society's Wolfson Research Merit Award. He is an enthusiastic supporter of industrial and academic liaison and he offers a range of industrial courses. He is also a Governor of the IEEE VTS. During 2008 - 2012 he was the Editor-in-Chief of the IEEE Press and a Chaired Professor also at Tsinghua University, Beijing. His research is funded by the European Research Council's Senior Research Fellow Grant. For further information on research in progress and associated publications please refer to http://www-mobile.ecs.soton.ac.uk Lajos has 20 000+ citations.